5-2012

Synergy of Alum and Chlorine Dioxide for Curbing Disinfection Byproduct Formation Potential at Central Arkansas Water

Corey W. Granderson
University of Arkansas, Fayetteville

SYNERGY OF ALUM AND CHLORINE DIOXIDE FOR CURBING DISINFECTION BYPRODUCT FORMATION POTENTIAL AT CENTRAL ARKANSAS WATER

SYNERGY OF ALUM AND CHLORINE DIOXIDE FOR CURBING DISINFECTION BYPRODUCT FORMATION POTENTIAL AT CENTRAL ARKANSAS WATER

A thesis submitted in partial fulfillment
of the requirements for the degree of
Master of Science in Civil Engineering

By

Corey W. Granderson
University of Arkansas
Bachelor of Science in Civil Engineering, 2008

May 2012
University of Arkansas

Abstract

Central Arkansas Water (CAW), the water utility for Little Rock, AR, draws their source water from Lake Maumelle and Lake Winona. To curb disinfection byproduct (DBP) formation, CAW has begun retrofitting their two plants to use chlorine dioxide as an alternative primary disinfectant followed by free chlorine secondary disinfection in the distribution system. In this study, fluorescence parallel factor (PARAFAC) analysis was combined with free chlorine simulated distribution system (SDS) tests and DBP formation potential (DBPFP) tests to study the benefit of chlorine dioxide primary disinfection (CDPD) with alum coagulation. Of the DBPs screened, trichloromethane (TCM) was formed in highest concentration in each source water and treatment scenario. In the DBPFP tests, TCM formation potential decreased on average by 30 and 42% after alum coagulation for Lake Maumelle and Lake Winona waters, respectively; after CDPD/alum coagulation, TCM formation potential decreased on average by 61 and 67%, indicating that CDPD was beneficial. Fluorescence-PARAFAC analysis identified four humic-like fluorophores with maximum intensity (F_{MAX}) values that were linearly correlated (r^2 values between 0.92-0.94) with the DBPFP of TCM; weaker linear correlations were found between TCM and chlorine demand ($r^2 = 0.41$) and TCM and $SUVA_{254}$ ($r^2 = 0.67$). The strong correlations between DBPFP and F_{MAX} indicate that fluorescence-PARAFAC analysis may be a useful screening tool to evaluate strategies (e.g., set chlorine dioxide and alum doses) to curb DBPs at CAW.

This thesis is approved for recommendation
to the Graduate Council.

Thesis Director:

_____

Dr. Julian L. Fairey

Thesis Committee:

_____

Dr. James C. Young

_____

Dr. Wen Zhang

Thesis Duplication Release

I hereby authorize the University of Arkansas Libraries to duplicate this thesis when needed for research and/or scholarship

Agreed _____

Corey W. Granderson

Refused _____

Corey W. Granderson

Acknowledgements

I would like to thank Julian Fairey for his guidance, meticulous review, and encouragement during my graduate studies. I would also like to thank Ashley Pifer for teaching me the laboratory methods used during this research, and for her help on many of the experiments and data analysis. I would like to thank Sarah Cousins, Dan Miskins, Samantha Hovis, and Clint Mash for their help in the laboratory as well. And thank you to my wife Callie for her patience and support through my graduate studies.

Table of Contents

List of Tables

List of Figures

Acronyms

CAW – Central Arkansas Water

CDPD – Chlorine dioxide primary disinfection

DBP – Disinfection byproduct

DBPFP – Disinfection byproduct formation potential

DCBM – Dichlorobromomethane

DWTP – Drinking water treatment plant

EEM – Excitation-emission matrix

F_{MAX} – maximum fluorescence intensity

NOM – Natural organic matter

PARAFAC – Parallel factor analysis

SDS – Simulated distribution system

$SUVA_{254}$ – Specific ultraviolet adsorption at 254-nm

TCM – Trichloromethane (chloroform)

THM – Trihalomethane

WRL – Water research laboratory

1. Introduction and Motivation

Source waters (i.e., lakes, rivers, groundwater) contain natural organic matter (NOM) that originates from allochthonous (i.e., soil runoff, subsurface leaching, leaf decay, etc.) and autochthonous (i.e., algae) sources. During drinking water disinfection, undesirable reactions between NOM and disinfectants (e.g., free chlorine) form disinfection by-products (DBPs) (Rook 1977). The United States Environmental Protection Agency (USEPA) regulated 11 DBPs (four trihalomethanes, five haloacetic acids, chlorite ion, and bromate) through the Stage 1 Disinfectants/ Disinfection Byproducts (D/DBP) Rule, which required the running annual average (RAA) trihalomethane (THM) and haloacetic acid (HAA) concentrations to be below the maximum contaminant level (MCL) of 80 and 60 μg L^{-1}, respectively. Between 2006-2010, the finished drinking water at Central Arkansas Water (CAW), the drinking water utility for the city of Little Rock, AR, has been approaching the MCL for THM, with some individual sampling sites in excess (86.5-114.0 μg L^{-1}) (Central Arkansas Water 2012). Water utilities have been preparing for the USEPA Stage 2 D/DBP Rule (promulgated in 2006 with required compliance by 2012-2016), which bases MCL compliance on *locational* RAAs for "worst-case-scenario" DBP-forming locations in a distribution system. In an attempt to curb DBP formation, CAW has begun retrofitting their two drinking water treatment plants (DWTPs) with chlorine dioxide primary disinfection (CDPD) facilities in place of free chlorine. This study is intended to assess the benefit of changing the primary disinfectant from free chlorine to chlorine dioxide in terms of THM formation.

Coagulation using metal salts such as aluminum sulfate (alum) has proven effective in drinking water treatment for reducing turbidity. In enhanced coagulation the optimal coagulant dose and pH are set based on the removal of total organic carbon (i.e., a surrogate of NOM used

to assess DBP formation). While targeting total organic carbon (TOC) has improved DBP control, a fraction of the DBP precursors remain that can react with disinfectants like free chlorine to form DBPs (Drikas et al. 2003).

Chlorine dioxide has been proven effective in deactivating bacteria, viruses, and parasites in source waters, and prevents algal growth in DWTPs (Miltner 1976, White 1999, Gagnon et al. 2006). In addition, chlorine dioxide has been used to oxidize metals such as iron and manganese and remove taste and odor causing compounds (White 1999, Arora et al. 2001, Gagnon et al. 2006). Miltner (1976) showed that mixtures of chlorine dioxide and free chlorine could reduce THM formation and that as the ClO_2:Cl_2 ratio increased for a simultaneous dose, THM formation decreased. He concluded that chlorine dioxide was not removing THMs or reacting with free chlorine, but rather reacting to reduce the concentration of DBP precursors.

Alam et al. (2008) coupled alum coagulation with CDPD and observed a small (but statistically significant) reduction in the ultraviolet absorption at 254 nm (UV_{254}), a parameter related to the aromatic content of NOM (Weishaar et al. 2003) which has been correlated with DBP formation. In the same study, no reduction in THM formation was observed in side-by-side pilot trains – one with CDPD, one without – after chlorinating in simulated distribution tests (SDS); however, the pilot plant utilized ozonation after coagulation/flocculation/settling processes which most likely hindered dissemination of any ClO_2-specific effects on THM formation (Alam et al. 2008). Because alum coagulation/flocculation/settling processes are impacted by the nature of NOM in a system (Win et al. 2000), chlorine dioxide pre-disinfection may indirectly impact these processes (Alam et al. 2008) because it is a more selective oxidant than free chlorine (Gates 1998). For example, Iriarte-Velasco et al. (2007) reported that another primary disinfectant, nascent chlorine (a variable mixture of free chlorine, ozone, and chlorine

dioxide generated in situ by electrolysis), favored the conversion of humic matter to non-humic matter, and suggested that this conversion to smaller particle size would have a deleterious effect on coagulation. It is unknown whether or not CDPD acts beneficially with alum in terms of curbing formation of DBPs.

THM formation is affected by DBP precursor concentration and reactivity and disinfectant type, dose, and contact time (Sorlini and Collivignarelli 2005). NOM, a primary group of DBP precursors, is a diverse pool of chemical moieties, and can undergo physical and chemical changes by biological processes (i.e., microbial decay) and photolysis. Further, seasonal changes and weather events can alter NOM quantity and reactivity (Huguet et al. 2009). Changes in these variables can shift the DBP formation and speciation and alter the effectiveness of control measures. At present, DWTPs evaluate NOM (and subsequently predict DBPFP) by measuring dissolved organic carbon (DOC) and calculating the specific ultraviolet absorbance at 254 nm ($SUVA_{254} = UV_{254}/DOC$). This non-specific parameter does not address the physical and chemical properties of NOM that are integral to predicting DBP formation and optimizing DBP precursor removal. In an attempt to improve the accuracy and consistency of NOM characterization, fluorescence excitation-emission matrices (EEMs) have been studied and found to correlate well to DBP precursor concentration. Pifer and Fairey (2012) used parallel factor analysis (PARAFAC) to decompose EEMs into principal fluorophore groups and demonstrated improved correlations relative to $SUVA_{254}$ between trichloromethane (the predominant THM) and fluorescence maximum intensity (F_{MAX}) values of a humic fluorophore group in chlorinated raw and alum-treated waters.

To comply with the Stage 2 D/DBP Rule, CAW has begun retrofitting its DWTPs to dose chlorine dioxide as a primary disinfectant – with subsequent free chlorine secondary disinfection

to maintain a distribution system residual. In this study, raw lake water samples were collected monthly (7/20/11-12/14/11) from the two CAW source reservoirs and side-by-side analyses were conducted to assess the benefit of chlorine dioxide and alum coagulation using disinfection byproduct formation potential (DBPFP) tests. These tests require a 3-5 mg L^{-1} total chlorine residual at pH7 after 7-days and are useful in evaluating the ultimate yield of DBP precursors. CAW source waters were alum coagulated with and without CDPD, chlorinated, and analyzed for DBPs. Additionally, EEMs created for raw and treated water samples were decomposed by fluorescence-PARAFAC analysis and F_{MAX} values compared to $SUVA_{254}$ for predicting DBP formation and control. The correlation between PARAFAC component removal and reduction in DBP formation following these treatments was investigated as an alternative to correlations of $SUVA_{254}$ and 7-day chlorine demand – both considered indicators of DBPFP. Additional goals during this study were to develop laboratory methods for chlorine dioxide generation and measurement capabilities for both chlorine dioxide and chlorite ion concentration. The goal of this research was *not* to determine an optimal chlorine dioxide dose or treatment regime as in a pilot scale study, but rather to determine the impact of chlorine dioxide for lowering DBPFP.

2. Methods and Materials

2.1. Sample collection and handling

Water samples were collected from two reservoirs west of Little Rock, Arkansas – Lake Maumelle, located on the Big Maumelle River, and Lake Winona, located on the Alum Fork of the Saline River. These reservoirs supply the source water for CAW, which serves approximately 400,000 customers. Lake Maumelle has a surface area of 36 km^2, average depth of 7.5 m, and is the source water for the Jack H. Wilson DWTP, which provides 60% of CAW's drinking water. Lake Winona has a surface area of 5 km^2, average depth of 10.5 m, and is the source water for the Ozark Point DWTP (this plant also receives raw water supplements from Lake Maumelle), and provides the remaining 40% of CAW's drinking water. Lake Maumelle's contributing watershed has an area of 35,612 ha and is situated within the *Maumelle River-Arkansas River* watershed. This watershed is mostly forest (90%) with 7-8% pastureland and 2-3% urban development. The Lake Winona watershed (*Headwaters Alum Fork Saline River*) has an area of 14,050 ha that is 93% forestland and <1% urban development. Raw water samples were collected monthly from three United States Geological Survey (USGS) sampling locations on each reservoir over a six-month period by the CAW staff (Table A1). Samples were collected headspace-free in 9-L HDPE carboys with screw-top lids and transported in coolers to the University of Arkansas Water Research Laboratory (WRL) and stored at 4°C in the dark until use.

All water for aqueous preparations and analyses at the WRL was made using a Millipore Integral 3 (Billerica, MA) Milli-Q water system (18.2 MΩ-cm) and ACS-grade chemical reagents. Glassware was scrubbed through a bath of Alconox detergent and tap water before

being rinsed three times with deionized water and three times with Milli-Q water. Glassware used for organics analyses was then baked in a muffle furnace at 400°C for a minimum of 30-min, while all other non-precision glassware was dried in a desiccator oven. Plastics and precision glassware were cleaned in the same manner but allowed to air-dry at room temperature. An aliquot of each raw water sample was filtered (1 μm nominal pore size glass fiber filter, pre-combusted at 400°C for 30-min and pre-rinsed with 1 L Milli-Q water) to remove particles and homogenize the samples for use in the water quality tests.

2.2. Water quality tests

The pH of the raw waters was measured using an Orion 8272 pH electrode (Thermo Orion, Waltham, MA) calibrated daily with pH standards of 4, 7, and 10 and connected to an Accumet XL60 dual channel pH/Ion/Conductivity meter. Alkalinity measurements were made according to Standard Methods 2320B, in which raw waters were titrated to a carbonic acid endpoint of pH 4.0 with 0.1-N HCl. TOC and dissolved organic carbon (DOC) were measured with a Tekmar Dohrmann Phoenix 8000 TOC analyzer (Mason, Ohio). UV_{254} was measured on a Shimadzu UV-Vis 2450 (Kyoto, Japan) spectrophotometer using a 1 cm path length low volume quartz cell. Specific ultraviolet absorbance ($SUVA_{254}$) values were calculated by dividing the UV_{254} by the product of the DOC and UV cell path length. Turbidity was measured on a HF Instruments DRT-100 turbidimeter (Fort Myers, Florida).

2.3. Chlorine dioxide synthesis

ClO_2 was synthesized following Pepich et al. (2007) by combining a sodium chlorite (Amresco, Solon, OH) solution (16 g in 100 mL) with a potassium persulfate (Macron Chemical, Center Valley, PA) solution (8 g in 200 mL) in a 500 mL gas-wash bottle (Wilmad-LabGlass,

Vineland, NJ) protected from room light. Nitrogen gas was sparged at approximately 250 mL min^{-1} through the gas-wash bottle for 30-min while the reaction proceeded. The outlet of the gas-wash bottle was connected to a glass tube with fritted disk submerged into a 1 L beaker containing 500 mL of pre-chilled Milli-Q water that was insulated with chilled ice packs and shielded from room light. Stock chlorine dioxide was immediately transferred to a pre-rinsed, 100 mL gas-tight syringe (SGE, Australia) and distributed to several 20 mL amber vials with PFTE-lined screw-top lids and stored headspace-free in the dark at 4ºC until analyzed. Chlorine dioxide stock concentrations were determined by dilution (<1.0 Abs. at 360 nm) with Milli-Q water and measurement on a spectrophotometer using an assumed molar absorptivity of 1225 cm^{-1} M^{-1}. This concentration was subsequently confirmed by USEPA Method 327.0 – Revision 1.1 (USEPA 2005).

2.4. Chlorite ion and chlorine dioxide measurement

USEPA Method 327.0 (EPA-327) – *Determination of chlorine dioxide and chlorite ion in drinking water using lissamine green B and horseradish peroxidase with detection by visible spectrophotometry* – was developed to confirm by dilution the concentration of synthesized chlorine dioxide stock solutions and measure chlorine dioxide and chlorite ion residuals in dosed waters.

Reagent preparation for EPA-327 was done with analytical grade stock chemicals. A concentrated citric acid/glycine buffer was prepared by combining 9 g trisodium citrate dehydrate (J.T. Baker, Phillipsburg, NJ), 5 g disodium hydrogencitrate sesquihydrate (Alfa Aesar, Ward Hill, MA), and 1.0 g glycine (J.T. Baker, Phillipsburg, NJ) in 125 mL of Milli-Q water and stored in an amber glass bottle. This reagent was preserved with one drop of chloroform and

refrigerated (4-6ºC) in the dark. 240 mg of lissamine green B (LGB; Acros Organics, New Jersey) was diluted to 250 mL with Milli-Q water and stirred overnight. Purity was confirmed by measuring the absorbance at UV_{633} following a 1% addition (v:v) of the concentrated citric acid/glycine buffer. A buffered LGB stock solution was created in reagent water consisting of 40% LGB concentrated stock and 6% concentrated citric acid/glycine buffer and preserved with one drop of chloroform. This solution was combined with a buffered horseradish peroxidase (HRP; MP Biomedicals, Solon, OH) stock solution to create a combined LGB/HRP reagent which was preserved with one drop of chloroform and considered stable for 14-days.

EPA-327 was followed to measure the chlorite ion concentration directly and chlorine dioxide concentration indirectly by difference using duplicate samples. For each water sample analyzed, duplicate 16 mL amber glass vials were prepared – one sparged with nitrogen (20-min at approximately 250 mL min^{-1}) using a Pasteur pipet, and one unsparged – and momentarily stored headspace-free. A 1.0 mL aliquot was wasted from each vial, and replaced with 1.0 mL of concentrated citric acid/glycine buffer solution, capped, and mixed. Then another 1.0 mL aliquot was wasted and replaced with 1.0 mL of the LGB/HRP reagent, capped, and mixed. The HRP rapidly converted chlorite ion to chlorine dioxide, which oxidized the LGB, thus reducing its absorption at UV_{633}. A standard curve was prepared using a 1000 mg L^{-1} chlorite ion stock solution (Ultra Scientific, North Kingstown, RI) between 0.20-2.00 mg L^{-1} (n=5, r^2=0.99).

2.5. Chlorine dioxide dosing and alum jar tests

Two treatment scenarios were analyzed in this study: SDS tests (7/20/11 and 8/10/11) and DBPFP tests (9/14/11-12/14/11). Dosing parameters and hold times for all tests are shown in Table A2. Samples collected on 7/20/11 and 8/10/11 were dosed according to the reservoir-

specific, in-situ treatment regime anticipated at their respective DWTP. Waters dosed with ClO_2 were held headspace free in 1 L amber glass bottles in the dark at room temperature before jar tests. Following ClO_2 hold time, all samples were adjusted to pH 5.7 and subsequently dosed with either 13 mg L^{-1} or 23 mg L^{-1} alum as $Al_2(SO_4)_3*14H_2O$ and a pre-determined amount of soda ash to preserve alkalinity. Alum and soda ash were injected simultaneously via disposable syringe into the jar test apparatus (Challenge Technology, Springdale, AR) with magnetic stir bars rotating at 200 rpm for 30-seconds to simulate rapid mixing. Stirring was reduced to 40-rpm during the 30-min flocculation, and then samples were allowed to settle for 30 minutes. Treated samples were then dosed with free chlorine and held for seven days prior to DBP analyses.

2.6. Disinfection by-product formation potential

DBPFP tests on filtered CAW water and jar test supernatant from 9/14/11-12/14/11 were performed in 250 mL amber glass bottles with PFTE-lined screw-top lids at pH 7 (phosphate buffer), stored at 25°C in the dark, and 3 to 5 mg L^{-1} total chlorine residual at 7-days. Concentration of stock NaOCl solution (Fisher Scientific, Fair Lawn, NJ) was determined following Standard Methods 4500-Cl B and diluted to create a 5 mg mL^{-1}-Cl_2 dosing solution. Standards between 0.5 and 10 mg L^{-1}-Cl_2 ($n = 5$, $r^2 = 0.99$) were prepared and analyzed using Hach DPD (Hach Company, Loveland, CO) powder pillows and a UV-spectrophotometer at 552 nm. After the 7-day hold time, each chlorinated sample was analyzed for seven DBPs: TCM (trichloromethane), TCAN (trichloroacetonitrile), DCAN (dichloroacetonitrile), DCBM (dichlorobromomethane), DBCM (dibromochloromethane), TBM (tribromomethane), and TCP (1,1,1-Trichloro-2-propanone). The DBPs were measured by liquid-liquid extraction using pentane and gas chromatography with an electron capture detector following EPA Method 551.1

on a Shimadzu GC-2010 (Kyoto, Japan). Standards (including a 1,1,1-trichloroethane internal standard) were prepared using certified solutions from AccuStandard, Inc. (New Haven, CT).

2.7. Fluorescence-PARAFAC analyses

Fluorescence excitation-emission matrices (EEMs) were collected for all filtered raw waters, alum coagulated waters, and CDPD/alum coagulated waters (68 samples) using a dual monochromator fluorescence detector (Agilent Technologies, Model G1321A). Two valid PARAFAC models were produced, a four and six component model, following Pifer et al. (2011). The six component model was chosen because it isolated a previously identified background noise component from the fluorescence detector (Pifer et al. 2011) more so than the four-component model. As such, five component fluorophores identified through PARAFAC were used in this study. Though only 12 raw water samples were chlorinated and analyzed for DBPs, the remaining 24 raw water sample EEMs were used to help the PARAFAC model validate. For each EEM and component fluorophore, the PARAFAC model produced a fluorescence maximum intensity value (F_{MAX}) that was used quantitatively to assess DBP formation and control.

3. Results and Discussion

3.1. Water quality parameters

Raw water quality parameters for the six sampling locations are summarized in Table 1, organized by sampling date. The raw waters were near-neutral pH throughout the testing period with a range of 6.1-7.4, with similar mean pH values in the two lakes (6.7 and 6.9). The alkalinities of these waters were low, with means of 13.6 and 11.5 mg L^{-1} as $CaCO_3$ for Lake Maumelle and Lake Winona, respectively. Given these low capacities, alkalinity would be consumed during alum addition, and therefore base (e.g., soda ash) was added simultaneously during the jar tests. Turbidities were very low during the entire testing period with a range of 0.6-6.0 NTU, a mean of 2.4 NTU, and no observed seasonal trends. $SUVA_{254}$ generally increased during the sampling period, with Lake Winona $SUVA_{254}$ consistently greater (average 5.6 L mg^{-1} m^{-1}) than that of Lake Maumelle (average 4.3 L mg^{-1} m^{-1}).

3.2. Chlorine dioxide disinfection byproducts

It has been well documented that treatment with chlorine dioxide alone will not form THMs, but reacts in aqueous solutions to form chlorite ion and chlorate, both DBPs. Chlorite ion is regulated at 1 mg L^{-1} by the USEPA under the Stage 2 D/DBP Rule. Several studies have reported chlorite ion yields to be between 30-70% of the consumed chlorine dioxide (Aieta et al. 1984, Werdehoff and Singer 1987, Gordon 1992, Baribeau et al. 2002, Korn et al. 2002, Alam et al. 2008). Schmidt et al. (2000) showed that this variation can be due to source water NOM characteristics. Here, chlorite yields averaged 30% of the chlorine dioxide consumed (Table A3). This result can be used to assess chlorite formation in CAW waters upon chlorine dioxide

addition and suggest chlorine dioxide doses in excess of 3 mg L^{-1} could result in violations of the chlorite ion MCL without subsequent treatment to remove chlorite.

3.3. Simulated distribution system tests

SDS tests were conducted on samples LMLI and LWR from the 7/20/11 and 8/10/11 sampling dates using the ClO_2, alum, and free chlorine doses and hold-times as noted in Table A2. Unexpectedly, $SUVA_{254}$ was higher after alum coagulation compared to the raw and CDPD/alum coagulated waters.

Only TCM and DCBM are reported in Figure 1 (panels *(a)* and *(b)* for SDS tests) because almost all other DBPs formed in concentrations near or below the method detection limit (MDL = 3 µg L^{-1}). In all four source waters and three treatment scenarios, TCM formed in the highest concentrations (30.2 to 67.6 µg L^{-1}). DCBM (3.8 to 9.3 µg L^{-1}) was also formed under all treatment scenarios, whereas DCAN was only formed in one raw water and three alum coagulated waters just above the MDL. DBCM, TCAN, TBM, and TCP were not detected in either of the source waters under any of the treatment scenarios. Overall, the LWR waters had higher total DBP formation, which was dominated by TCM (>91%). Because DCBM was formed at low concentrations, discussion of the trends in formation reduction was limited to TCM.

No significant temporal differences were observed per reservoir during the SDS tests. On average, alum coagulation decreased TCM in the LMLI waters by 6.7 µg L^{-1} (14% reduction). Similarly, alum coagulation decreased TCM in LWR waters by 11.7 µg L^{-1} on average (18% reduction). For the LMLI waters, CDPD/alum coagulation further decreased TCM by 10 µg L^{-1} on average. In contrast, in the LWR SDS tests, CDPD/alum coagulation did not decrease TCM

formation, indicating that either ClO_2 may not be beneficial for TCM reduction in all water sources, or that for this water source the oxidation of NOM by 1 mg $L^{-1}$of ClO_2 was insufficient to lower the chlorine demand of the water to 1.5 mg L^{-1} or less. In the latter case, all free chlorine would be utilized and maximum TCM formation would be limited by free chlorine – not by precursor reactivity or concentration. At these low doses of chlorine dioxide and free chlorine it was not possible to draw conclusions as to the benifit between chlorine dioxide and alum coagulation.

3.4. Disinfection byproduct formation potential tests

To assess the impacts of CDPD in terms of curbing DBPs, DBPFP tests were conducted. Here, neither chlorine dioxide nor free chlorine were limiting reagents and DBP formation was limited by precursor (i.e., NOM) concentration and reactivity. During the DBPFP experiments, the source water location for Lake Maumelle reservoir was changed from LMLI to LMN (*Lake Maumelle near Natural Steps, AR*) because this sampling location is closer to the intake structure for the Jack H. Wilson DWTP.

For all DBPFP tests, $SUVA_{254}$ decreased 37% and 46% on average by alum coagulation and CDPD/alum coagulation, respectively (Table A2). In all eight source waters and each treatment scenario, TCM was the predominant DBP at concentrations between 31.7 to 171.0 µg L^{-1}, as shown in Figure 1. By month and treatment scenario, Lake Winona waters formed higher TCM concentrations than Lake Maumelle. Compared to chlorinated raw waters, alum coagulation reduced TCM concentrations by an average of 28 and 63 µg L^{-1} (30% and 42% reduction) in Lake Maumelle and Lake Winona waters, respectively. Similarly, CDPD/alum coagulation reduced TCM formation in Lake Maumelle and Lake Winona waters by 57 and 98

μg L^{-1} (61% and 67% reduction), respectively. This indicates the benefit of CDPD and alum coagulation for removal of TCM precursors. The increase in alum dose from 13 to 23 mg L^{-1} in the LMN waters did not improve TCM formation potential reduction, and therefore no benefit would be gained by dosing alum in excess, including during the CDPD/alum coagulation regime.

DCBM was formed in second-greatest concentration (3.0 to 10.0 μg L^{-1}) for all samples, but was below the MDL in a number of cases. DBCM, TBM, and TCAN were not detected above the MDL in any of the DBPFP tests. Chlorinated LWR raw water samples formed small amounts of DCAN (3.1 to 4.7 μg L^{-1}), but DCAN was not detected in any samples after alum coagulation with or without CDPD. Measureable amounts of TCP (3.0 to 4.1 μg L^{-1}) were only formed in a handful of alum-coagulated samples.

Both the 5.7 and 8.2 mg L^{-1} chlorine dioxide doses reduced TCM formation potential by 60 ± 3% and 66 ± 6% on average, respectively. Chlorine dioxide selectively oxidizes NOM in source water, and even when dosed in great excess (8.2 mg L^{-1}) there is still NOM available to react with free chlorine that was non-reactive with chlorine dioxide. This supports the hypothesis that not all NOM was oxidized by chlorine dioxide, but only a specific fraction of NOM species due to its selective nature (Gates 1998). In addition, because no increased formation was observed as the chlorine dioxide dose increased, further investigation is required to determine the optimum chlorine dioxide dose between 1 and 5.7 mg L^{-1} for the CAW waters.

3.5. Fluorescence-PARAFAC analyses

The PARAFAC numerical model identified a valid 6-component model using 65 EEMs (3 of the raw waters were identified as outliers). One of these components had been previously identified as instrument noise (Component 6 – Figure A1) and was discarded for subsequent

analyses. Each of the five remaining components was identified in Table 2 with corresponding excitation and emission maxima. Upon comparison of excitation and emission loading plots (Figure A2) with literature-reported fluorophores (Coble 1996, Hall and Kenny 2007, Dubnick et al. 2010, Pifer et al. 2011, Pifer and Fairey 2012), Components 1, 2, 4, and 5 were identified as humic-like fluorophore groups and Component 3 was identified as a protein-like group. Figure 2 shows the F_{MAX} values for Components 1-5 for raw waters and alum coagulated waters both with and without CDPD. The sum of F_{MAX} intensities for all five components was greatest for the raw water samples as compared to the treated waters. By sampling date, LWR raw waters had higher F_{MAX} intensities per component than the Lake Maumelle waters. Consistent F_{MAX} reduction occurred during the DBPFP tests for each humic-like component (1, 2, 4, and 5) due to alum coagulation (mean reductions of 70%, 54%, 23%, and 48%, respectively) with increased reduction following CDPD/alum coagulation (mean reductions of 89%, 76%, 53%, and 69%, respectively) (Table 3). Consistently higher reduction of F_{MAX} for Components 1 and 2 was observed in LMN waters when alum dose was increased from 13 to 23 mg L^{-1}. During the DBPFP tests, reduction of precursor material – quantified as fluorescence-PARAFAC Components 1-5 (Figure 2) – mirrored the subsequent reduction in TCM formation potential upon chlorination (Figure 1).

Table 3 shows the average percent contribution of each component, which is dominated by F_{MAX} for Components 1 (27%) and 2 (32%) in the raw waters. After alum coagulation, the major components were 3 and 4 which were least affected by this treatment, as indicated by the lowest percent reductions. Component 3 (protein-like) was the least reduced fluorophore group during alum coagulation, but was subsequently reduced 50% on average by CDPD/alum coagulation. An explanation for this observation is that chlorine dioxide selectively oxidized

these protein-like fluorophores that did not settle out in alum floc. Average percent reductions of specific components after alum coagulation varied from 8-70% (Components 3 and 1, respectively). Using CDPD/alum coagulation, an approximate 20% increase in average percent reduction was observed for humic-like components.

3.6. Correlations between TCM formation and NOM properties

The four humic-like component fluorophore groups, identified by the PARAFAC model, proved to be strong predictors of TCM formation potential in raw waters and alum-coagulated waters with and without CDPD. Figure 3 shows correlations between TCM formed during DBPFP tests regressed with chlorine demand and $SUVA_{254}$ (panels *(a)* and *(b)*, respectively) and F_{MAX} intensities for PARAFAC Components 1, 2, 4 and 5 (panels *(c)-(f)*, respectively). Poor correlations were observed between TCM formation and chlorine demand ($r^2 = 0.41$) and $SUVA_{254}$ ($r^2 = 0.67$). There were strong correlations between F_{MAX} for PARAFAC Components 1 and 4 and TCM formation potential (r^2 values of 0.94 and 0.93, respectively). F_{MAX} for PARAFAC Components 2 and 5 also has a strong correlation to TCM formation, with r^2 values of 0.92 and 0.93, respectively, but appear (visually) to have an initially steep slope that tapers-off past intensity values of 0.5. Protein-like Component 3 did not correlate well with DBP formation ($r^2 = 0.30$), most likely because proteins were not strong TCM precursors. Based on the correlations in Figure 3, F_{MAX} for PARAFAC Components 1, 2, 4 and 5 could be used to accurately assess TCM precursor concentrations in both reservoirs and to compare the effectiveness of different treatment regimes in curbing TCM formation.

4. Conclusions

SDS and DBPFP tests on raw and alum coagulated waters with and without CDPD, coupled with fluorescence-PARAFAC analyses, provided the following insights:

- An average chlorite ion yield of 30% after 24-hours resulted from chlorine dioxide doses of 5.7 and 8.2 mg L^{-1}.
- A chlorine dioxide dose of 1 mg L^{-1} did not curb DBP formation in the SDS tests.
- The optimum chlorine dioxide dose for the CAW waters studied was between 1 and 5.7 mg L^{-1}.
- TCM was the predominant DBP formed upon chlorination of Lake Winona and Lake Maumelle waters.
- Fluorescence-PARAFAC analyses identified four humic-like fluorophore groups and one protein-like fluorophore group in Lake Winona and Lake Maumelle.
- In the DBPFP tests, TCM formation potential decreased 30 and 42% on average after alum coagulation for Lake Maumelle and Lake Winona waters, respectively; after CDPD/alum coagulation, TCM formation potential decreased on average by 61 and 67%.
- F_{MAX} intensities for PARAFAC Components 1, 2, 3, and 4 were lowered by CDPD/alum coagulation on average by 20% beyond the reduction following alum coagulation alone.

- Humic-like PARAFAC components 1, 2, 4, and 5 had stronger correlations (r^2 values of 0.94, 0.92, 0.93, and 0.93, respectively) to TCM formation potential than either chlorine demand ($r^2 = 0.41$) or $SUVA_{254}$ ($r^2 = 0.67$).

Table 1. Water quality parameters for each sample date (7/20/11-12/14/11) and location.

Sampling Date	Sample Location	pH	Turbidity (NTU)	Alkalinity[a] (mg L^{-1}-$CaCO_3$)	DOC[b] (mg L^{-1}-C)	SUVA[c] (L mg^{-1} m^{-1})
7/20/2011	LME[d]	7.2	3.3	14.0	3.85	2.13
	LMLI[e]	7.4	2.2	15.0	3.31	2.27
	LMN[f]	7.3	1.6	14.5	4.38	1.69
	LWG[g]	7.0	1.4	12.0	5.75	2.42
	LWS[h]	7.0	2.2	13.0	5.25	3.07
	LWR[k]	7.2	1.4	12.5	4.24	3.16
8/10/2011	LME	6.6	6.0	12.5	2.14	3.88
	LMLI	6.6	2.4	12.0	1.86	3.71
	LMN	6.8	2.2	12.5	1.89	3.54
	LWG	6.8	1.6	9.8	2.84	4.33
	LWS	6.1	3.0	11.5	2.83	5.48
	LWR	6.6	1.6	10.0	2.77	4.44
9/14/2011	LME	7.0	3.0	14.8	2.01	3.43
	LMLI	6.9	1.5	14.5	1.94	3.45
	LMN	6.7	1.2	15.5	1.88	3.46
	LWG	6.6	1.4	11.5	3.10	3.94
	LWS	6.5	1.2	12.5	3.06	3.99
	LWR	6.7	1.4	11.3	3.04	3.98
10/12/2011	LME	6.7	1.4	14.8	0.98	6.12
	LMLI	7.1	1.0	15.3	1.01	5.84
	LMN	7.3	1.3	16.5	1.04	5.48
	LWG	7.1	0.6	14.8	1.35	6.89
	LWS	6.4	0.9	11.5	1.35	8.30
	LWR	6.7	0.6	13.3	1.49	6.64
11/9/2011	LME	6.7	2.5	14.0	1.36	4.12
	LMLI	6.6	1.8	13.4	1.24	4.35
	LMN	6.8	4.2	13.3	1.18	4.58
	LWG	6.6	2.1	11.1	1.55	6.58
	LWS	6.4	4.0	11.0	1.55	6.71
	LWR	6.6	2.0	11.5	1.58	6.52
12/14/2011	LME	6.5	5.2	10.5	1.84	8.04
	LMLI	6.6	3.5	11.5	1.54	5.91
	LMN	6.9	3.3	11.3	1.48	4.93
	LWG	7.1	3.9	11.0	1.86	7.74
	LWS	6.4	4.2	9.0	1.31	8.85
	LWR	6.5	3.7	10.0	1.92	7.81
Mean Values ± Standard Deviations						
Lake Maumelle		6.9 ± 0.3	2.6 ± 1.4	13.6 ± 1.6	1.9 ± 1.0	4.3 ± 1.6
Lake Winona		6.7 ± 0.3	2.1 ± 1.2	11.5 ± 1.4	2.6 ± 1.3	5.6 ± 2.0

[a] Endpoint pH=4.0; [b] Dissolved organic carbon; [c] Specific ultraviolet absorption calculated as (UV_{254}/DOC×Cell path length); [d] Lake Maumelle east of Hwy 10 bridge near Wye, AR; [e] Lake Maumelle near Little Italy, AR; [f] Lake Maumelle at Natural Steps; [g] Lake Winona DS from Gillis Branch near Reform, AR; [h] Lake Winona DS from Stillhouse Creek near Reform; [k] Lake Winona at Reform, AR.

Table 2. Maxima location and characteristics of fluorescence-PARAFAC components.

PARAFAC Component	Excitation Maxima (nm)	Emission Maxima (nm)	Identification
1	258 (333)	456	Humic-like (Coble 1996, Hall and Kenny 2007)
2	234 (308, 384)	420	Humic-like (Coble 1996, Pifer et al. 2011)
3	230 (280)	351	Protein-like (Dubnick et al. 2010, Pifer and Fairey 2012)
4	344 (250)	426	Humic-like (Coble 1996, Pifer and Fairey 2012)
5	391 (227, 280)	489	Humic-like (Pifer et al. 2011)

Values in parentheses are secondary and tertiary excitation maxima.

Table 3. Average percent contribution and percent reduction of each fluorescence-PARAFAC component as a result of alum coagulation with and without chlorine dioxide pre-disinfection in DBPFP tests (9/14/11-12/14/11).

Treatment	Component 1	Component 2	Component 3	Component 4	Component 5
Average Contribution					
Raw	27 ± 3	32 ± 4	18 ± 8	11 ± 1	11 ± 2
Alum	15 ± 2	28 ± 7	31 ± 9	16 ± 1	11 ± 1
ClO_2 + Alum	10 ± 2	27 ± 8	32 ± 10	19 ± 2	12 ± 2
Average Percent Reduction					
Alum	70 ± 5	54 ± 10	8 ± 10	23 ± 8	48 ± 9
ClO_2 + Alum	89 ± 4	76 ± 9	50 ± 10	53 ± 8	69 ± 8

Values are averages ± standard deviations.

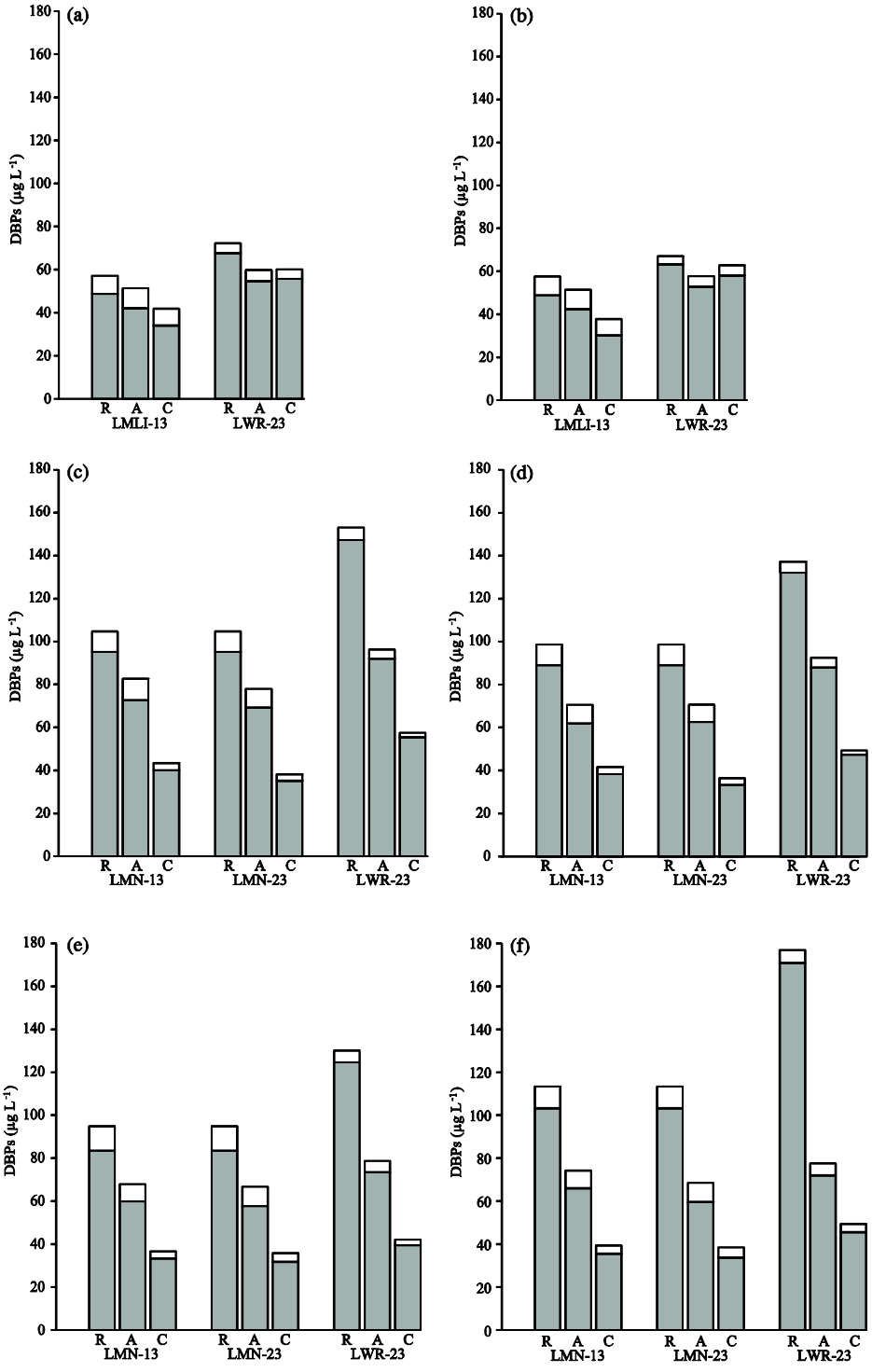

Figure 1. Disinfection byproducts (DBPs) in µg L^{-1} formed during simulated distribution tests ((*a)* 7/20/2011 & *(b)* 8/10/2011) and DBP formation potential tests ((*c)* 9/14/2011, *(d)* 10/12/2011, *(e)* 11/9/2011, and *(f)* 12/14/2011) with free chlorine for each treatment scenario. R

represents a raw water sample, A represents an alum coagulated water sample, and C represents an alum coagulated sample pre-disinfected with chlorine dioxide. LMLI-13 is Lake Maumelle near Little Italy, AR water dosed at 13 mg L^{-1} alum, LWR-23 is Lake Winona at Reform, AR water dosed at 23 mg L^{-1} alum, and LMN-13 and LMN-23 are Lake Maumelle at Natural Steps water dosed at 13 and 23 mg L^{-1} alum, respectively. DBPs are indicated as follows: ■ trichloromethane and □ dichlorobromomethane.

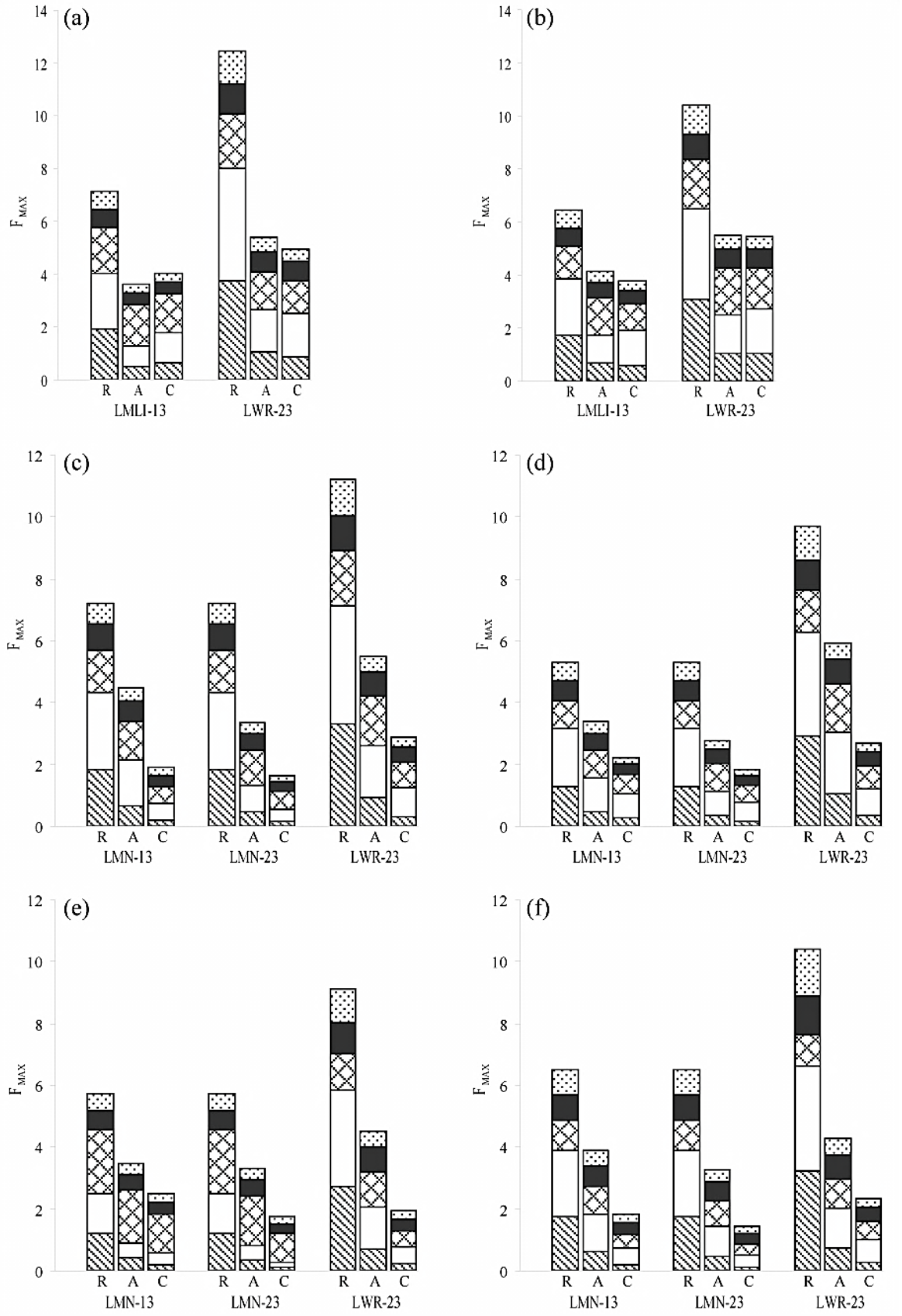

Figure 2. Fluorescence-PARAFAC component maximum intensities (F_{MAX}) per sampling dates: (a) 7/20/2011, (b) 8/10/2011, (c) 9/14/2011, (d) 10/12/2011, (e) 11/9/2011, and (f) 12/14/2011. R represents a raw water sample, A represents an alum coagulated water sample, and C represents an alum coagulated sample pre-disinfected with chlorine dioxide. LMLI-13 is Lake Maumelle near Little Italy, AR water dosed at 13 mg L^{-1} alum, LWR-23 is Lake Winona at Reform, AR water dosed at 23 mg L^{-1} alum, and LMN-13 and LMN-23 are Lake Maumelle at Natural Steps water dosed at 13 and 23 mg L^{-1} alum, respectively. Fluorescence-PARAFAC components are indicated as follows: ▧Component 1, □ Component 2, ⊠ Component 3, ■ Component 4, and ▩ Component 5.

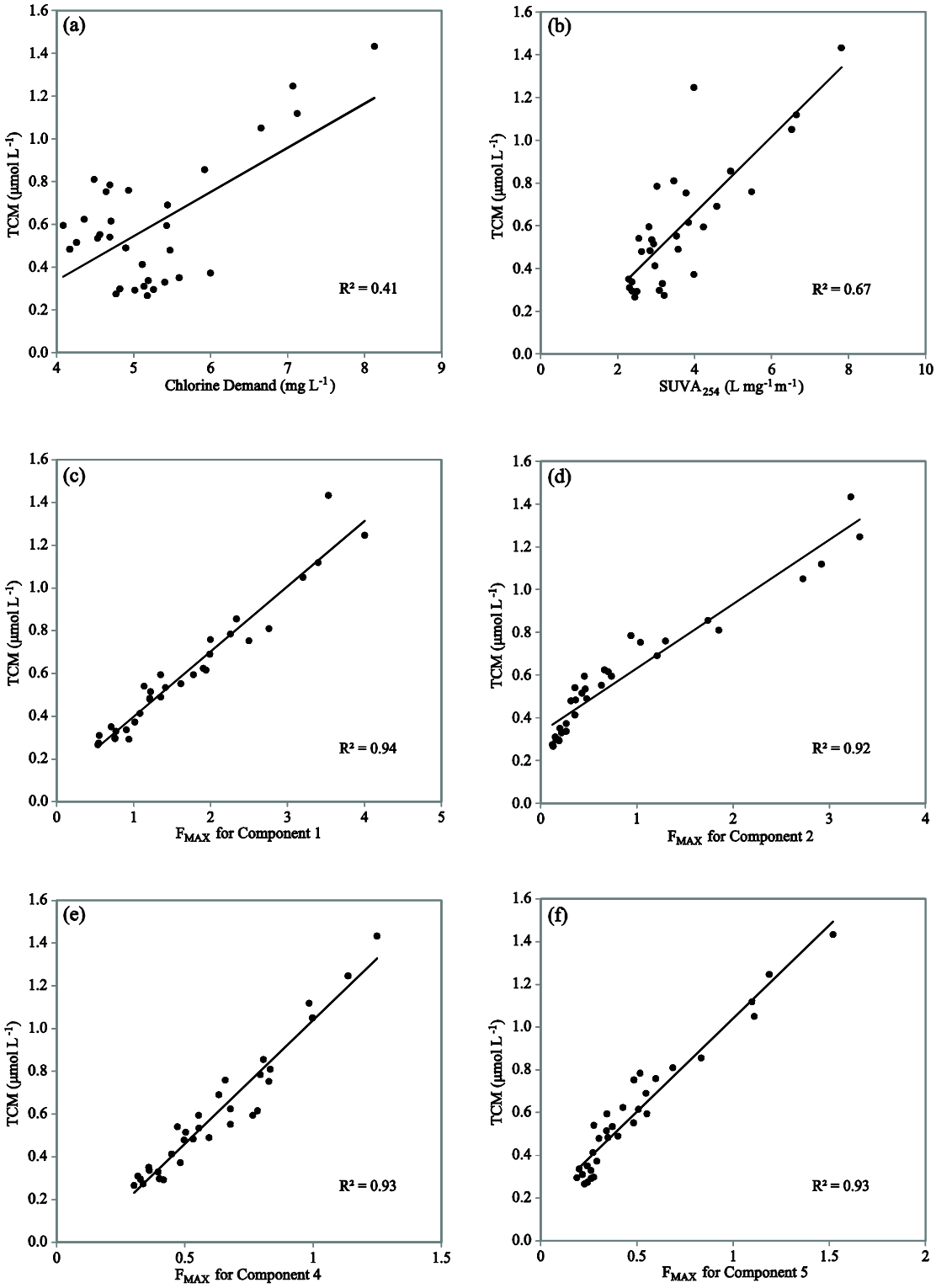

Figure 3. Correlations between trichloromethane (TCM in µmol L^{-1}) formed during free chlorine DBP formation potential tests and (a) chlorine demand, (b) $SUVA_{254}$, (c) F_{MAX} for Component 1, (d) F_{MAX} for Component 2, (e) F_{MAX} for Component 4, and (f) F_{MAX} for Component 5.

References

Central Arkansas Water (2012). *2006-2010 Water Quality Reports*. Accessed Online, http://www.carkw.com/source/water_quality_reports.asp.

United States Environmental Protection Agency (2005). "*Method 327.0 - Determination of chlorine dioxide and chlorite ion in drinking water using lissamine green B and horseradish peroxidase with detection by visible spectrophotometry*." Revision 1.1.

Aieta, E. M., P. V. Roberts and M. Hernandez (1984). "Determination of chlorine dioxide, chlorine, chlorite, and chlorate in water." *Journal American Water Works Association* **76**(1): 64-70.

Alam, M. Z. B., R. E. Cantwell, R. Hofmann, R. C. Andrews, J. L. Rand, G. A. Gagnon, M. VanderMarck, E. Moffat and S. A. Andrews (2008). "Effect of ClO(2) pretreatment on subsequent water treatment processes." *Journal of Environmental Engineering-ASCE* **134**(6): 478-485.

Arora, H., M. LeChevallier and D. Battigelli (2001). "Effectiveness of chlorine dioxide in meeting the enhanced surface water treatment and disinfection by-products rules." *Journal of Water Supply Research and Technology-Aqua* **50**(4): 209-227.

Baribeau, H., M. Prevost, R. Desjardins, P. Lafrance and D. J. Gates (2002). "Chlorite and chlorate ion variability in distribution systems." *Journal American Water Works Association* **94**(7): 96-105.

Coble, P. G. (1996). "Characterization of marine and terrestrial DOM in seawater using excitation emission matrix spectroscopy." *Marine Chemistry* **51**(4): 325-346.

Drikas, M., C. W. K. Chow and D. Cook (2003). "The impact of recalcitrant organic character on disinfection stability, trihalomethane formation and bacterial regrowth: An evaluation of magnetic ion exchange resin (MIEX (R)) and alum coagulation." *Journal of Water Supply Research and Technology-Aqua* **52**(7): 475-487.

Dubnick, A., J. Barker, M. Sharp, J. Wadham, G. Lis, J. Telling, S. Fitzsimons and M. Jackson (2010). "Characterization of dissolved organic matter (DOM) from glacial environments using total fluorescence spectroscopy and parallel factor analysis." *Annals of Glaciology* **51**(56): 111-122.

Gagnon, G., C. J. Volk, C. Chauret, H. M. Murphy, K. C. O'Leary and R. C. Andrews (2006). "Changes in microbiological quality in model distribution systems after switching from chlorine or chloramines to chlorine dioxide." *Journal of Water Supply Research and Technology-Aqua* **55**(5): 301-311.

Gates, D. (1998). *The chlorine dioxide handbook*. Denber, American Water Works Association.

Gordon, G. (1992). Water chemistry of the oxy-chlorine species. *Proc. Second International Symposium on Chlorine Dioxide: Drinking Water Issues*. Houston, TX, American Chemistry Council.

Hall, G. J. and J. E. Kenny (2007). "Estuarine water classification using EEM spectroscopy and PARAFAC-SIMCA." *Analytica Chimica Acta* **581**(1): 118-124.

Huguet, A., L. Vacher, S. Relexans, S. Saubusse, J. M. Froidefond and E. Parlanti (2009). "Properties of fluorescent dissolved organic matter in the Gironde Estuary." *Organic Geochemistry* **40**(6): 706-719.

Iriarte-Velasco, U., J. I. Alvarez-Uriarte and J. R. Gonzalez-Velasco (2007). "Removal and structural changes in natural organic matter in a Spanish water treatment plant using nascent chlorine." *Separation and Purification Technology* **57**(1): 152-160.

Korn, C., R. C. Andrews and M. D. Escobar (2002). "Development of chlorine dioxide-related by-product models for drinking water treatment." *Water Research* **36**(1): 330-342.

Miltner, R. J. (1976). The effect of chlorine dioxide on trihalomethanes in drinking water. *College of Engineering*. Cincinnati, OH, University of Cincinnati. **Master of Science**.

Pepich, B. V., T. A. Dattilio, P. S. Fair, D. J. Munch, G. Gordon and Z. Kortvelyesi (2007). "An improved colorimetric method for chlorine dioxide and chlorite ion in drinking water using lissamine green B and horseradish peroxidase." *Analytica Chimica Acta* **596**(1): 37-45.

Pifer, A. D. and J. L. Fairey (2012). "Improving on SUVA(254) using fluorescence-PARAFAC analysis and disinfection byproduct formation and control." *Water Research*. DOI: http://0-dx.doi.org.library.uark.edu/10.1016/j.watres.2012.03.002.

Pifer, A. D., D. R. Miskin, S. L. Cousins and J. L. Fairey (2011). "Coupling asymmetric flow-field flow fractionation and fluorescence parallel factor analysis reveals stratification of dissolved organic matter in a drinking water reservoir." *Journal of Chromatography A* **1218**(27): 4167-4178.

Rook, J. J. (1977). "Chlorination reactions of fulvic acids in natural-waters." *Environmental Science & Technology* **11**(5): 478-482.

Schmidt, W., U. Bohme, F. Sacher and H. J. Brauch (2000). "Minimization of disinfection by-products formation in water purification process using chlorine dioxide - Case studies." *Ozone-Science & Engineering* **22**(2): 215-226.

Sorlini, S. and C. Collivignarelli (2005). "Trihalomethane formation during chemical oxidation with chlorine, chlorine dioxide and ozone of ten Italian natural waters." *Desalination* **176**(1-3): 103-111.

Weishaar, J. L., G. R. Aiken, B. A. Bergamaschi, M. S. Fram, R. Fujii and K. Mopper (2003). "Evaluation of specific ultraviolet absorbance as an indicator of the chemical composition and reactivity of dissolved organic carbon." *Environmental Science & Technology* **37**(20): 4702-4708.

Werdehoff, K. S. and P. C. Singer (1987). "Chlorine dioxide effects on THMFP, TOXFP, and the formation of inorganic by-products." *Journal American Water Works Association* **79**(9): 107-113.

White, G. C. (1999). *Handbook of Chlorination and Alternative Disinfectants, 4th edition*. New York, Wiley Interscience.

Win, Y. Y., M. U. Kumke, C. H. Specht, A. J. Schindelin, G. Kolliopoulos, G. Ohlenbusch, G. Kleiser, S. Hesse and F. H. Frimmel (2000). "Influence of oxidation of dissolved organic matter (DOM) on subsequent water treatment processes." *Water Research* **34**(7): 2098-2104.

Appendix

Table A1. Sampling location information for Central Arkansas Water.

USGS[a] Site Name	Abbreviation	USGS Site Id
Lake Maumelle		
Lake Maumelle East of Hwy 10 bridge near Wye, AR	LME	07263297
Lake Maumelle near Little Italy, AR	LMLI	07263299
Lake Maumelle at Natural Steps, AR[b]	LMN	072632995
Lake Winona		
Lake Winona DS from Gillis Branch near Reform, AR	LWG	07362589
Lake Winona DS from Stillhouse Creek near Reform, AR	LWS	07362588
Lake Winona at Reform, AR[b]	LWR	07362590

[a] United States Geological Survey; [b] This sample location was closest to the reservoir intake structure.

Table A2. All treatment scenarios with associated DBP concentration, UV_{254}, $SUVA_{254}$, and percent reduction in TCM formation potential for simulated distribution tests (7/20/11 & 8/10/11) and disinfection byproduct formation potential tests (9/14/11-12/14/11).

Date	Sample Location	Treatment Doses (mg L^{-1})			DBP Concentration			UV_{254} (au)[e]	$SUVA_{254}$ (L mg^{-1} m^{-1})[e]	TCM Reduction (%)
		ClO_2[a]	Alum[b]	Cl_2	TCM[c] (µg L^{-1})	DCBM[d] (µg L^{-1})	24-hr ClO_2^- (mg L^{-1})[e]			
7/20/11	LMLI[f]	-	-	1.5	48.8	8.4	-	0.075	3.93	-
	LMLI	-	13	1.5	42.0	9.3	-	0.031	5.85	14
	LMLI	1 (5hr)	13	1.5	34.1	7.8	NR[g]	0.028	4.31	30
	LWR[h]	-	-	1.5	67.6	4.7	-	0.134	4.56	-
	LWR	-	23	1.5	54.7	5.1	-	0.043	6.52	19
	LWR	1 (8hr)	23	1.5	55.8	4.4	NR	0.038	5.51	18
8/10/11	LMLI	-	-	1.5	48.9	8.7	-	0.069	3.71	-
	LMLI	-	13	1.5	42.4	9.0	-	0.032	5.42	13
	LMLI	1 (5hr)	13	1.5	30.2	7.5	NR	0.028	3.89	38
	LWR	-	-	1.5	63.2	3.8	-	0.123	4.44	-
	LWR	-	23	1.5	52.8	4.9	-	0.045	5.70	17
	LWR	1 (8hr)	23	1.5	58.1	4.8	NR	0.041	5.47	8
9/14/11	LMN[k]	-	-	10	96.7	9.7	-	0.065	3.46	-
	LMN	-	13	10	74.4	10.0	-	0.034	NR	23
	LMN	5.7	13	10	41.7	3.5	1.3	0.027	2.29	57
	LMN	-	23	10	70.9	8.9	-	0.027	2.81	27
	LMN	5.7	23	10	36.9	3.2	1.3	0.024	2.31	62
	LWR	-	-	10	148.7	6.1	-	0.121	3.98	-
	LWR	-	23	10	93.6	4.5	-	0.039	3.02	37
	LWR	5.7	23	10	57.1	BD[m]	1.4	0.038	2.62	62
10/12/11	LMN	-	-	10	90.5	9.9	-	0.057	5.48	-
	LMN	-	13	10	63.7	8.9	-	0.030	2.88	30
	LMN	5.7	13	10	40.1	3.5	1.0	0.028	2.37	56
	LMN	-	23	10	64.5	8.3	-	0.025	2.55	29
	LMN	5.7	23	10	35.2	3.3	1.0	0.024	2.38	61
	LWR	-	-	10	133.5	5.5	-	0.099	6.64	-
	LWR	-	23	10	89.8	4.8	-	0.037	3.78	33
	LWR	5.7	23	10	49.2	BD	1.2	0.038	2.97	63
11/9/11	LMN	-	-	10	82.3	9.5	-	0.054	4.58	-
	LMN	-	13	10	61.4	8.2	-	0.027	2.93	25
	LMN	8.2	13	10	34.9	3.4	1.0	0.027	2.50	58
	LMN	-	23	10	57.6	8.2	-	0.025	2.84	30
	LMN	8.2	23	10	31.7	3.2	1.0	0.023	2.45	62
	LWR	-	-	10	125.3	5.0	-	0.103	6.52	-
	LWR	-	23	10	73.4	4.4	-	0.033	3.84	41
	LWR	8.2	23	10	39.3	BD	1.7	0.031	3.16	69
12/14/11	LMN	-	-	10	102.1	8.2	-	0.073	4.93	-
	LMN	-	13	10	65.8	7.5	-	0.030	3.53	36
	LMN	8.2	13	10	35.4	3.0	1.6	0.029	3.09	65
	LMN	-	23	10	58.4	7.0	-	0.025	3.57	43
	LMN	8.2	23	10	32.6	BD	1.6	0.026	3.21	68
	LWR	-	-	10	171.0	5.9	-	0.150	7.81	-
	LWR	-	23	10	70.9	3.6	-	0.033	4.23	59
	LWR	8.2	23	10	44.4	BD	2.4	0.037	3.98	74

[a] Chlorine dioxide hold time was 24-hr except when noted in parenthesis; [b] mg L^{-1} as $Al_2(SO_4)_3*14H_2O$; [c] Trichloromethane; [d] Dichlorobromomethane; [e] Measurements in these columns were made before chlorination; [f] Lake Maumelle near Little Italy, AR; [g] Not reported; [h] Lake Winona at Reform, AR.; [k] Lake Maumelle at Natural Steps; [m] Below minimum detection level of 3 µg L^{-1}.

Table A3. Chlorine dioxide consumption and chlorite formation 24-hours after dosing.

Date	Location	ClO_2 Dose (mg L^{-1})	24-hr ClO_2 Residual (mg L^{-1})	ClO_2 Consumed (mg L^{-1})	24-hr ClO_2^- (mg L^{-1})	ClO_2^- Formed / ClO_2 Consumed
9/14/11	LMN	5.7	0.68	5.02	1.34	0.27
9/14/11	LWR	5.7	1.33	4.37	1.43	0.33
10/12/11	LMN	5.7	2.62	3.08	0.99	0.32
10/12/11	LWR	5.7	1.93	3.77	1.23	0.33
11/9/11	LMN	8.2	3.42	4.78	0.98	0.20
11/9/11	LWR	8.2	2.53	5.67	1.73	0.31
12/14/11	LMN	8.2	3.24	4.96	1.60	0.32
12/14/11	LWR	8.2	1.54	6.66	2.44	0.37

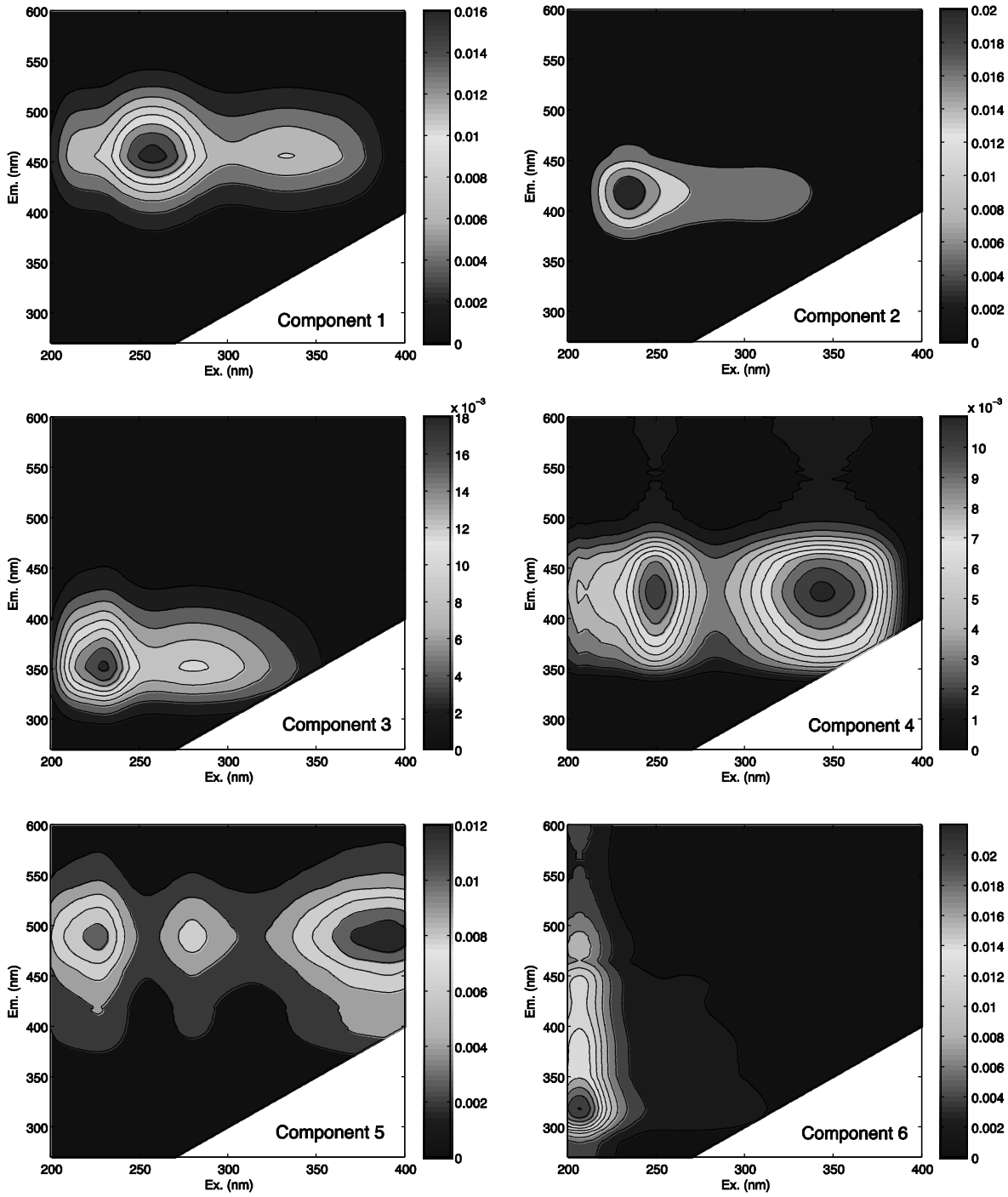

Figure A1. Fluorescence Components 1-6 identified using the PARAFAC model shown as excitation-emission matrices (EEMs).

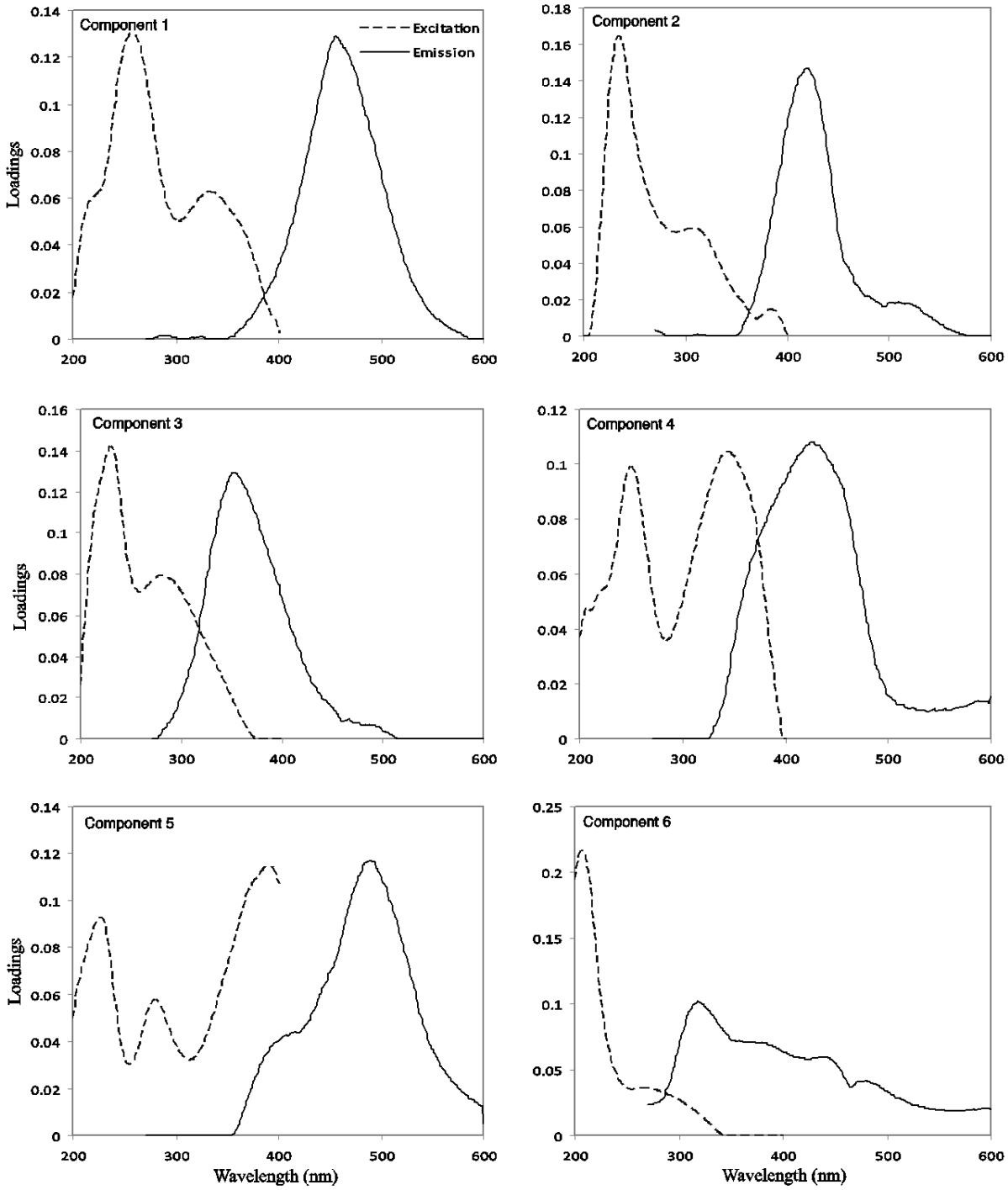

Figure A2. Fluorescence Components 1-6 identified using the PARAFAC model shown as excitation and emission loadings as a function of wavelength.